A Preliminary Analysis of Long Island Sound (LIS) Optical Cruise* May 2004

Dirk Aurin
University of Connecticut
Marine Sciences Department, Avery Point
Composed and Presented at:
Ocean Optics and Radiative Transfer Summer 2004

*Scientific crew included Heidi Dierssen, Mike Twardowski, Alison Branco
Funding: Steve Ackleson, Office of Naval Research (ONR)

Motivation

- To improve our understanding of the inherent optical properties (IOPs) of Long Island Sound estuary.
- To better parameterize the composition, structure, and ecology of LIS using the latest available technology in ocean optics and remote sensing.
- Generate a forward model of the apparent optical properties (AOPs) for one cruise station at the mouth of the estuary.
- Work toward optimizing inversion models of measured remote sensing reflectance (Rrs) to retrieve AOPs and biogeochemically significant information radiometrically.

Setting

East of New York City, NY, and surrounded by dense northeastern megolopolis, the LIS stretches 177 km roughly east-west and is 34 km wide at the widest point. It's average depth is 23.7 m. Fresh water entering the estuary flows in mainly from the Connecticut River, which flows southward through central CT from its origins in Canada 640 km to the north.

Western LIS increasingly suffers from eutrophically induced hypoxia each summer, which is aggrevated by anthropogenic nutirent loading. Because of its size and the density of the surrounding population, the Sound could greatly benefit from accurate interpretation of ocean color imagery collected from space. Remote retrievals of chlorophyll, chromophoric dissolved material (CDM), and particulate minerals coupled with recent advances in our ability to resolve the vertical structure of the residual tidal flow and transport across the coastal ocean boundary may be used as inputs to improve LIS ecosystem models in the future. This could impact resource and environmental protection policy, large, fragile commercial fisheries, and advances in carbon cycling research and pollution monitoring and abatement.

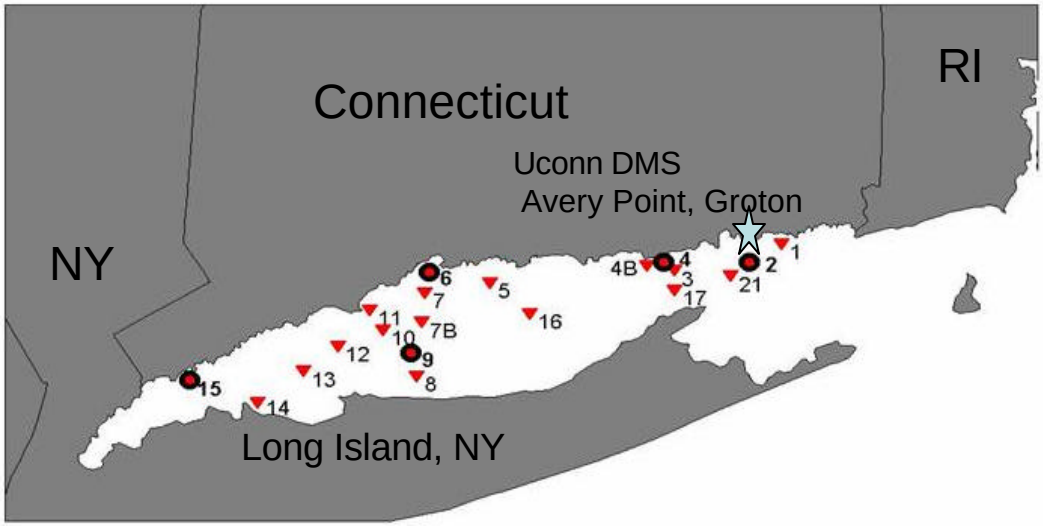

Figure 1. Stations for which forward and inverse models were run 2, 4, 21. Only results from 2 are presented here.

Figure 2. Local Area Coverage MODIS chlorophyll approximation for May 11; day one of the cruise. This is a single MODIS pass processed by NASA to Level 1A, and not a multi-day composite.

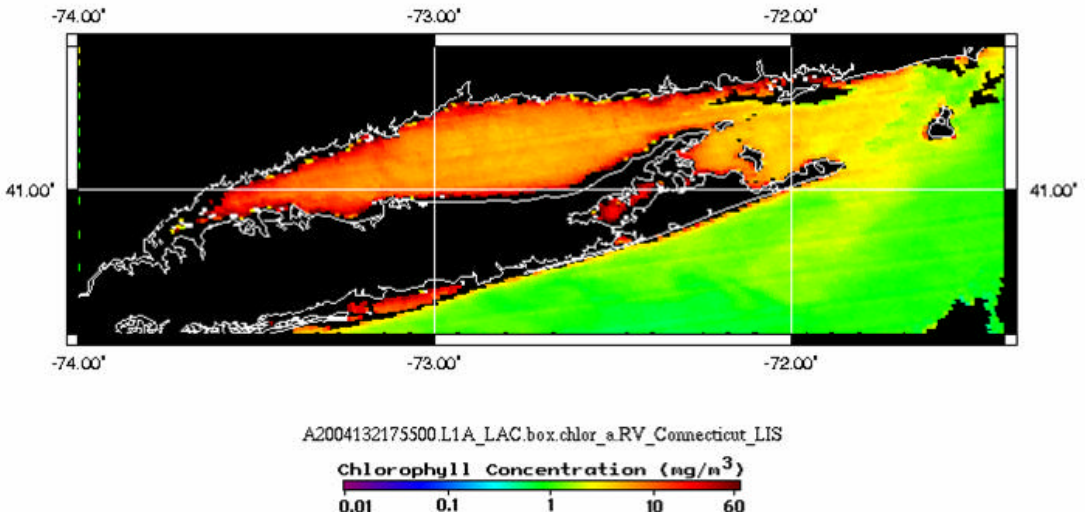

Platform and Instrumentation

R/V Connecticut

From left, Wet Labs President Casey Moore, NASA's Dr. Richard Miller and Wet Labs' Mike Twardowski, principal investigator of the project, prepare to lower a prototype of the Dolphin instrument into waters off the coast of Narragansett, R.I.

Photo courtesy of January edition NASA Stennis Newsletter: www.ssc.nasa.gov

Wetlabs, Inc. Ac-9

1. DOLPHIN (Diving Optical Profiler and High-speed Integration Network). A towed profiling instrument platform.
2. Dual AC-9s for simultaneaous measurement of whole- and dissolved water (0.2 µm pore size filter) absorption and attenuation.
3. BB3 single angle backscatter sensor for 3 spectral bands (470, 530, 650 nm)
4. BB2C single angle backscatter sensor for 2 spectral bands (530, 650 nm) and CDM fluorescence
5. SAM (Scattering Attenuation Meter) for backscatter at 650 nm
6. "Calibrated" Multi-spectral OCR-507 (7 band) in-water radiometer pair (Lu & Ed)
7. "Calibrated" Hyperspectral Analytical Spectral Device (ASD) (512 bands)

ASD

BB3

IOPs

All IOP data were collected using a Wetlabs DH4 logger aboard the DOLPHIN, and extraction from the DH4 was done by Wetlabs, Inc. Temperature, salinity and spectrally varying scattering corrections were applied to AC-9 data. Near surface measurements at station 2 were extracted and binned by depth and median filtered to remove outlier noise.

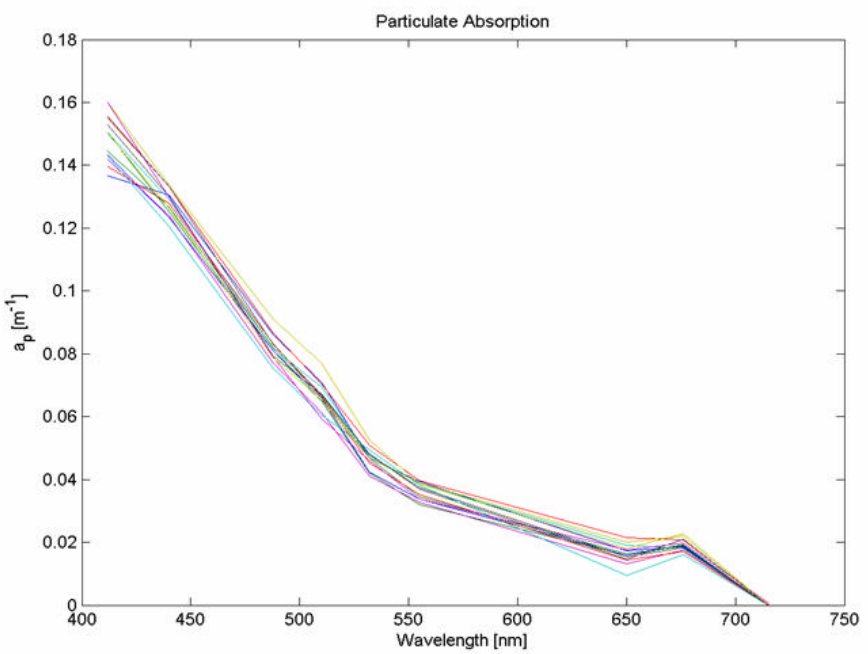

Figure 3. Spectrally varying total particulate absorption. The low absorption peak at 676 nm indicates a very weak signal for phytoplankton photosynthetic absorption. Colored plot lines indicate spectra from individual depth bins from 60 to 200 cm depth.

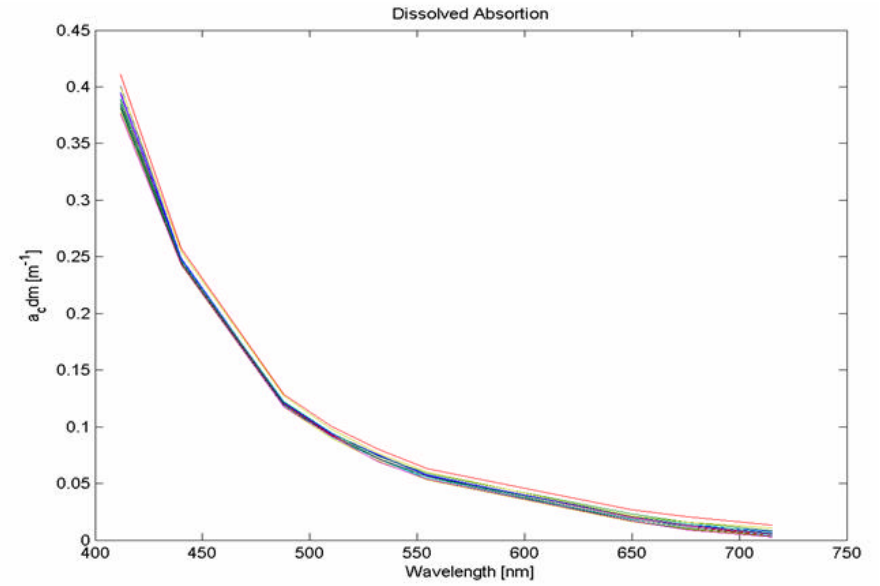

Figure 4. CDM absorption dominates total particulate absorption (Figure 4) by a factor of ~4 in the blue and ~2 in the red.

IOPs and Constituents

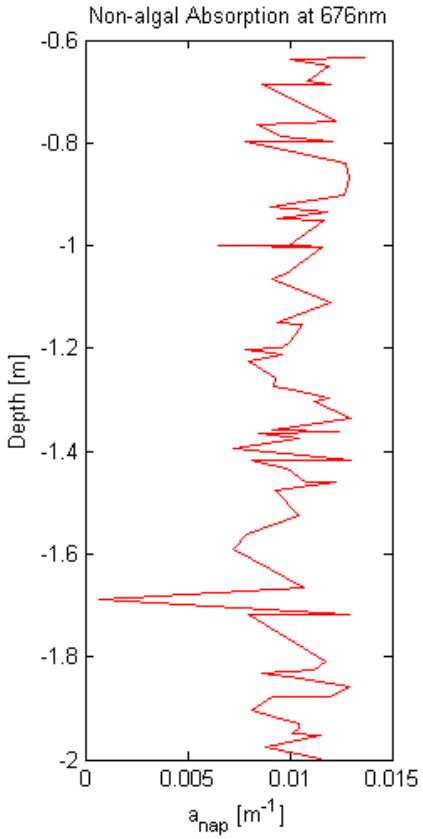

Figure 5. A profile of absorption by non-algal particles at 676 nm shows an average value of 0.010 ± 0.002 m^{-1}.

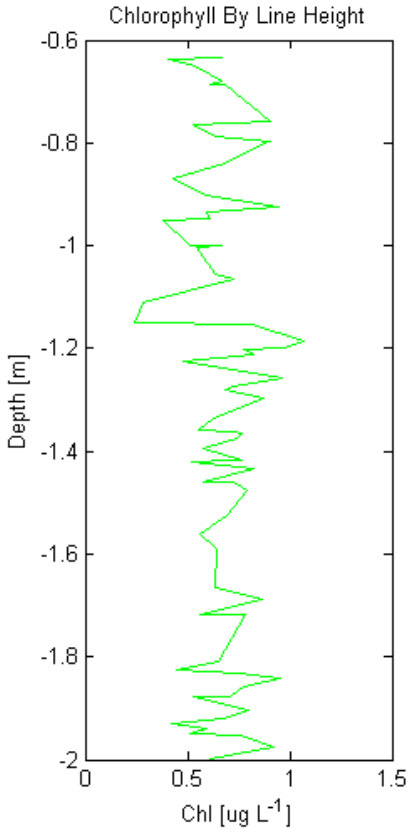

Figure 6. Estimated profile for chlorophyll-a with an average value of 0.676 ± 0.165 µg L^{-1}.

Chlorophyll-a (figure 6) was estimated by particulate absorption line-height ratio:

$a_?(676)$ =

$a_p(676) – \{[(a_p(650) - a_p(715)) / (650-715)] * (676-715) \}$

Absorption line-height ratio calculates the absorption due to phytoplankton at 676 nm, from which chl-a can be estimated from the empirically derived ratio:

chlorophyll = $a_?(676)$ /0.014

$a_?(676)$ can also be used to derive the non-algal contribution to absorption by subtracting it from the measured particulate absorption (figure 5).

A microscopist at the Univerisity of Rhode Island who added nutrients to water samples collected during the cruise described the water as, “remarkably devoid of life.” Further analysis of water sample collection is pending.

IOPs; Backscatter

Comparison for instrument agreement between the BB3, BB2F, and SAM reveals good agreement for backscatter and backscatter fraction (b_b/b) magnitude, but slight disagreement for spectral shape between 530 and 650 nm. Lack of instrument redundancy for backscatter at 470 nm may indicate that the steepening of the slope from -0.006 between 530 and 650 nm to -0.011 between 470 and 530 nm may not be trustworthy. In the following forward model analysis, however, backscatter was used from the BB3 for all three wavebands.

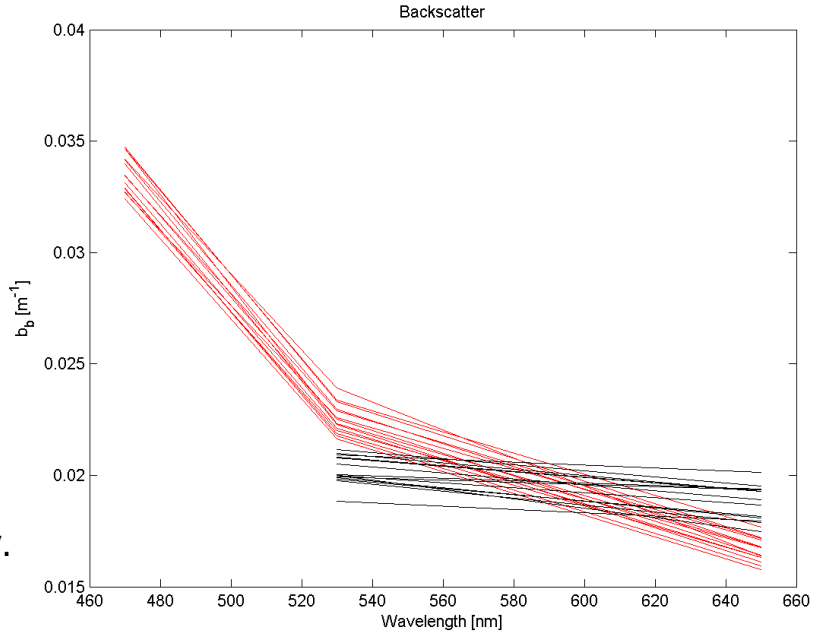

Figure 7. Spectral backscatter with binned BB3 data are shown here in red, and BB2C in black.

Overall backscatter fraction was about 2.5% (see figure 8) for all instruments. This seems to indicate a high proportion of minerals present in the water column which have a higher backscatter ratio than algae.

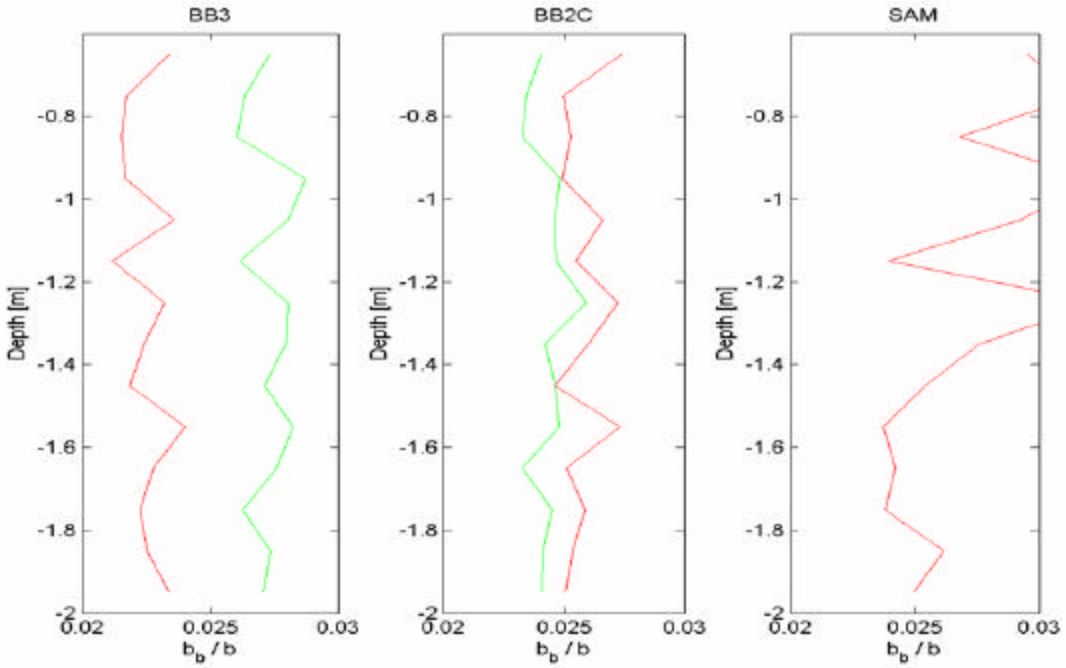

Figure 8. Backscatter ratio from BB3, BB2C, and SAM at 530 nm (green lines) and 650 nm (red). The first two instruments agree to what appears to be the instrument noise level, with $b_b = 0.0025 \pm 0.00085$. Only the SAM profile shows signal drift along the profile, yielding $b_b = 0.0273 \pm 0.0032$.

AOPs; Modeling the Light Field with Hydrolic

Model Parameters:

The Hydrolight model for AOPs was run to a depth of 10 m, with output AOPs for every 2 m at a 5 nm wavelength interval.

Sky Conditions
5/11/04
GMT 14.63
Lat. 41.2542
Lon. -72.1258
50% Overcast

Included elastic and inelastic scattering:
Chl fluorescence,
CDM fluorescence,
Raman scattering.

Measured IOPs input in model:
$a_{pg}(z)$ and $a_g(z)$ from AC-9, chl-a(z) from line-height estimation, and $b_b(z)$ at 470, 530, 650nm from BB3.

Figure 9. Diffuse attenuation coefficient of the upwelling irradiance (K_{lu}) as a function of depth and wavelength. The modeled value for K_{lu} is later used in one approach for L_u extrapolation to just below the sea-surface interface (see figure 19).

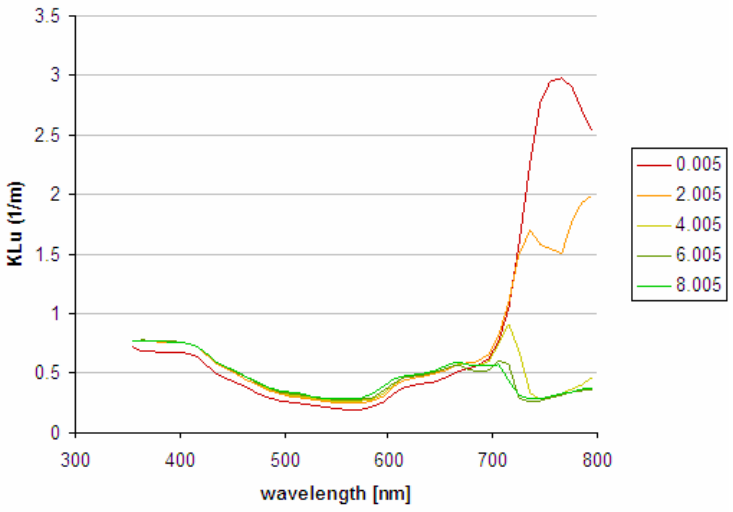

Figure 10. The remote sensing reflectance modelled from Hydrolight. The spectral shape indicates a green peak in the backscatter at 555 nm, and weak chlorophyll fluorescence at 685 nm.

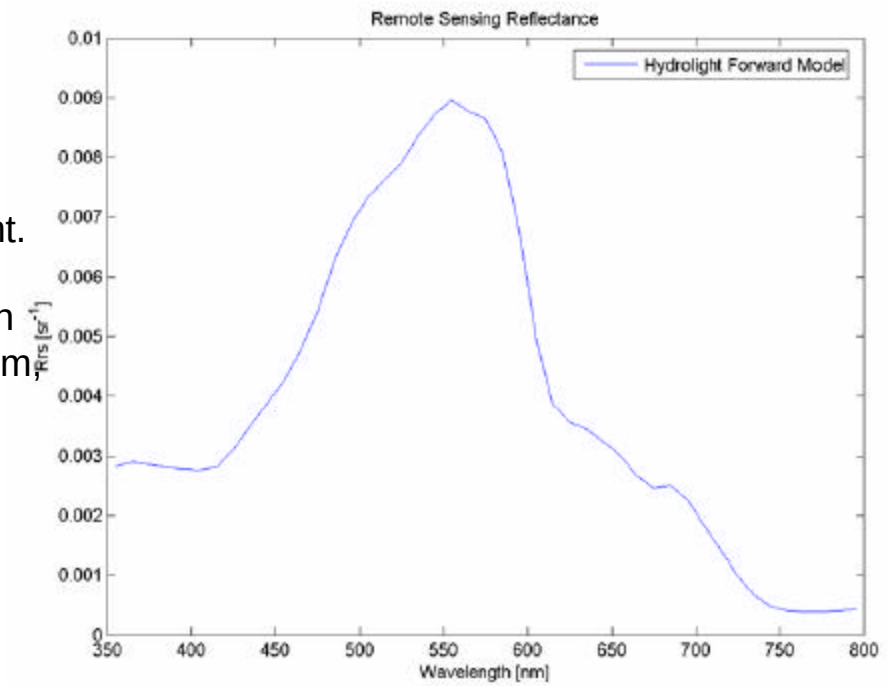

Optimizing the Roesler Perry (1995) Inverse Model

In the second stage of the project, the downwelling radiance at the sea-surface and water-leaving irradiance above the surface as measured from the Analytical Spectral Device (ASD) radiometers was used to estimate remote sensing reflectance at station 2. This reflectance spectrum was used as an input to the Roesler and Perry (1995) semi–analytical inversion model for the retrieval of IOPs including backscatter by small and large particles, absorption by CDM and non-algal particles, and constituents such as chlorophyll concentration. Model basis vectors for particulate backscatter, a_{nap} , a_{cdm}, and phytoplankton community parameterization were optimized using an iterative method for minimizing the root mean square error (RMSE) between the modelled and input Rrs.

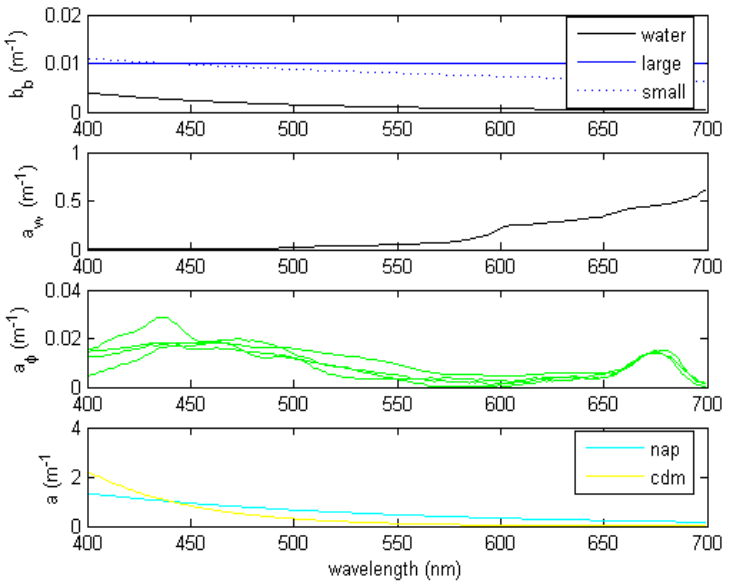

Figure 11. Optimized basis vectors applied to the inversion model showing spectrally flat particulate backscatter, Pope and Fry (1997) absorption for pure water adjusted to temperature 15° C and 33 psu, an empirical model for phytoplankton community distribution, and the exponential slopes for the specific absorption by non-algal particles and CDM.

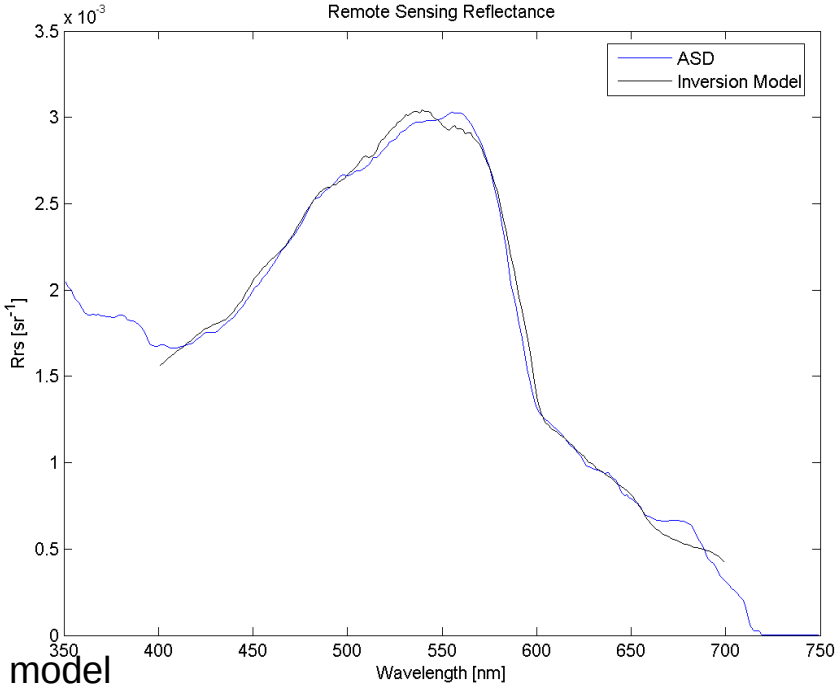

Figure 12. Measured and modelled Rrs for the best fit yielding a RMSE of 6.182 x 10^{-5}.

Seeking Inversion Closure; Measured vs. Modelled

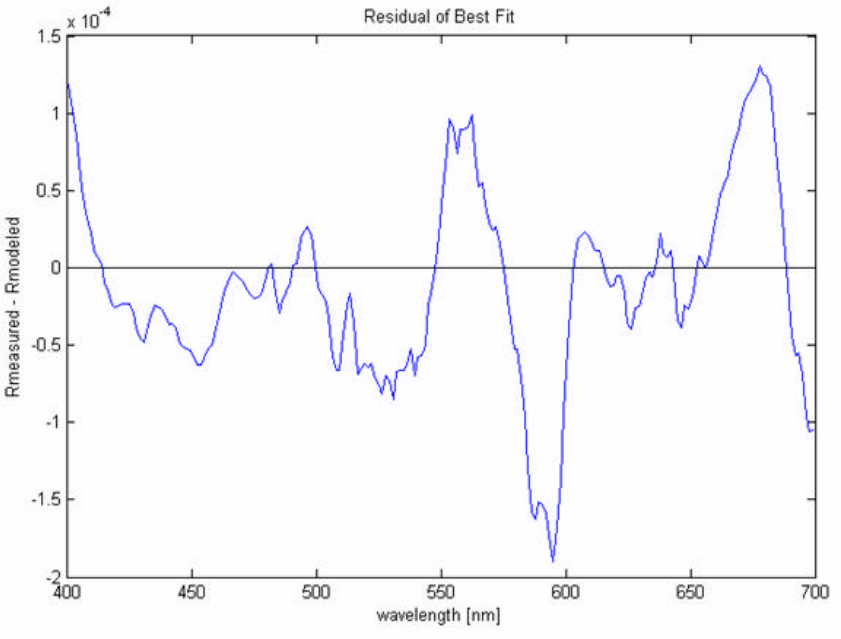

Figure 13. The residual for the optimal inversion model for Rrs shows the features of the measured reflectance spectrum for which the model could not accurately account. The largest deviation at 676 nm is an anticipated error due to the lack of a chlorophyll fluorescence term in the model. Deviations between 550 and 600 nm are likely due to slight mismatches between the pigment structure of the phytoplankton in the model versus those at station 2. A peak in the residual at 440 nm, and the small negative deviation at slightly higher wavelengths is due to the imperfect optimization for the exponential slope of CDM absorption (figure 14).

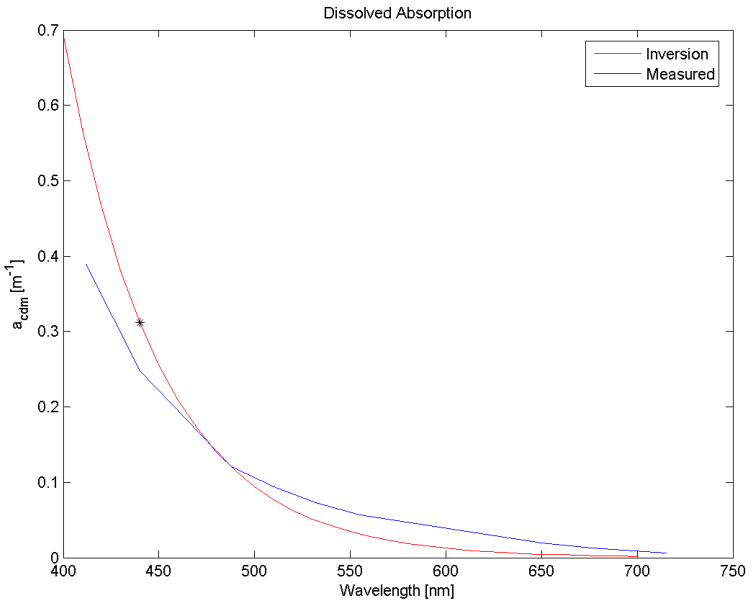

Figure 14. The difference between the measured CDM absorption and a reconstruction of the modelled a_{CDM} from $a_{CDM}(676)$ (shown as a black dot) shows that although the model could be slightly improved by a better choice for the exponential slope, an exponential may not be the best function for the model in this case.

Seeking Closure

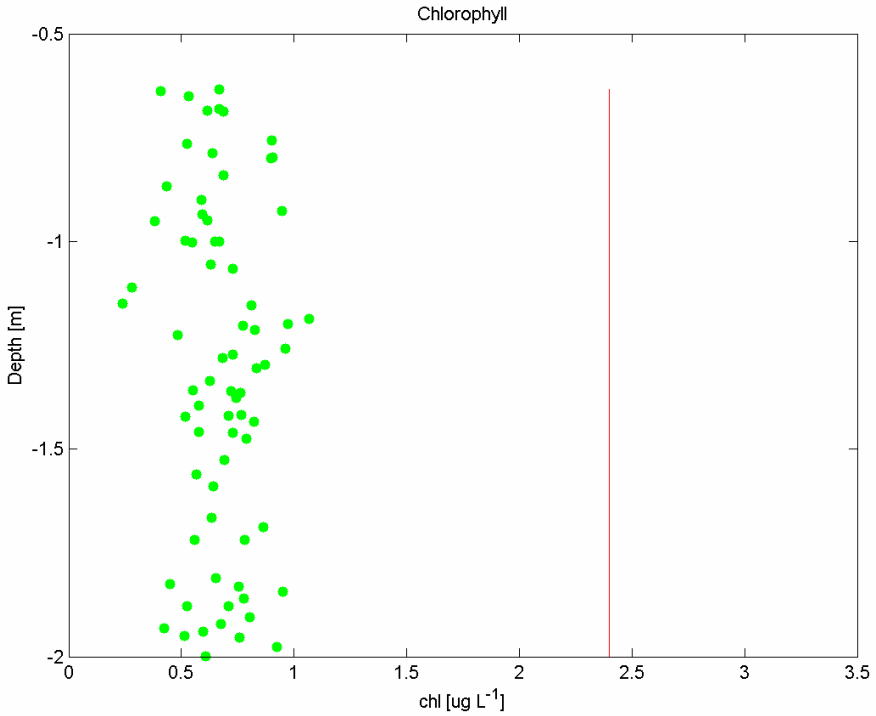

Figure 15. The estimated chlorophyll value from the model (2.4 µg L^{-1}, red line) disagrees with the estimated chlorophyll profile from AC-9 (green dots) by a factor of 3.55. The reason for the poor agreement is likely a result of problems with the radiometrically estimated Rrs rather than AC-9 instrument error, poor line-height approximation, or inversion model innaccuracy.

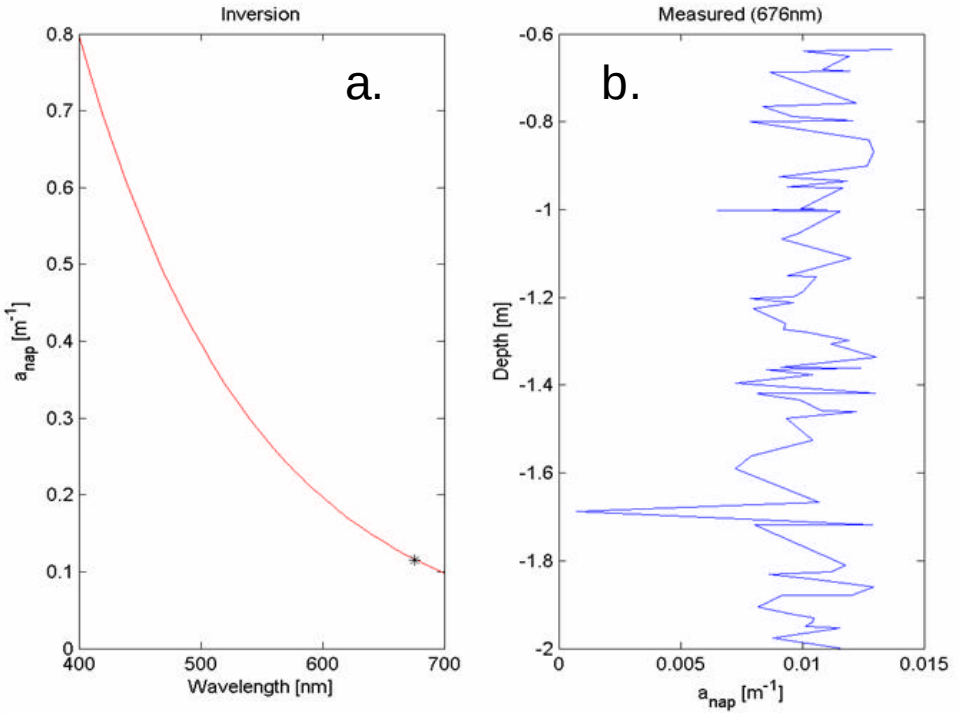

Figure 16 (a and b). a. A reconstruction of the modelled non-algal absorption from $a_{nap}(676)$ (black dot). b. The estimated non-algal component of absorbtion at 676 nm by line-height ratio. The two values differ by a factor of 11.6, throwing the validity of radiometric measurement into serious question.

Comparison of Inversion to Forward Model

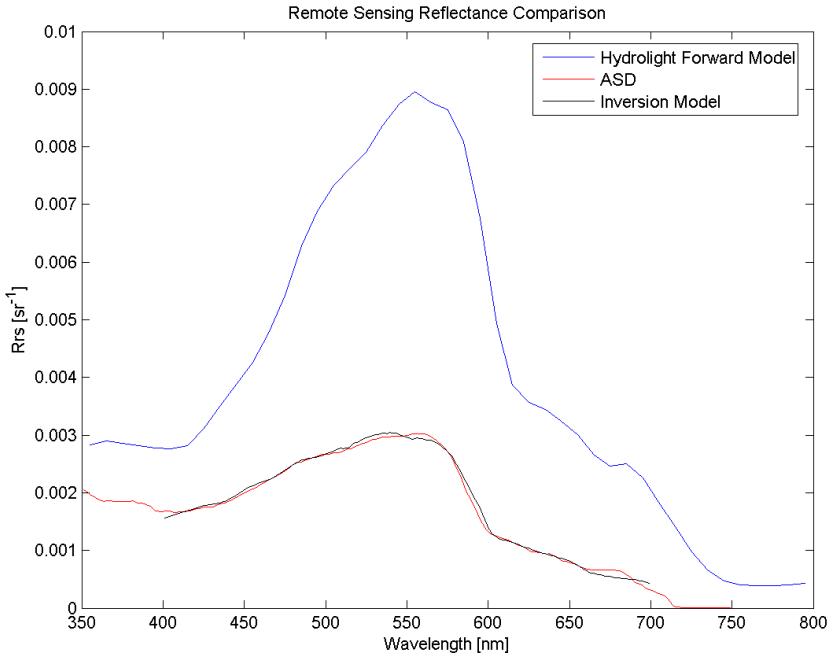

Figure 17. Although some similarities can be seen in the spectral shapes of the radiometric and modelled Rrs, the magnitudes differ by a factor of 3 at peak reflectance (555 nm).

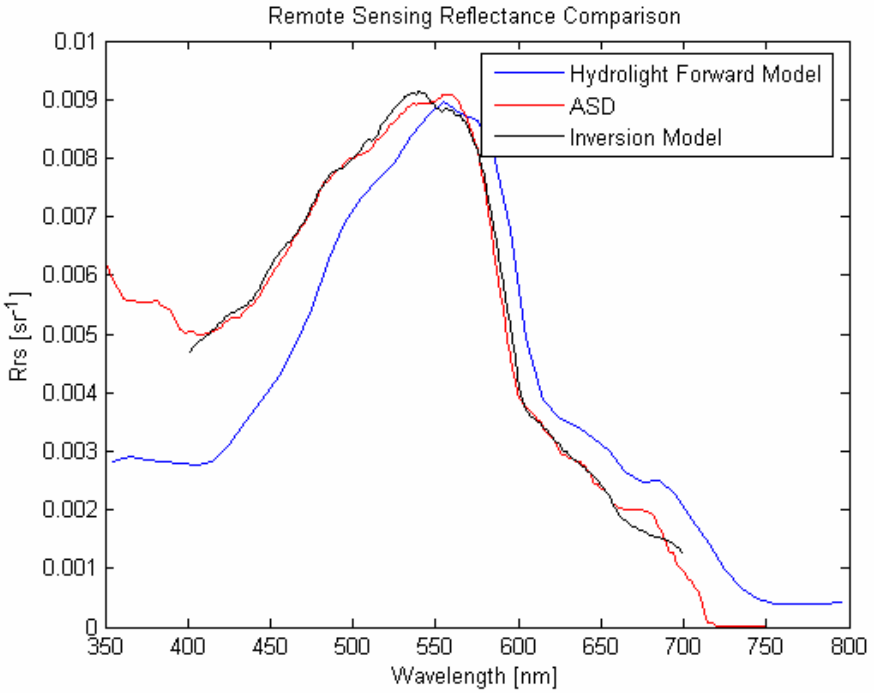

Figure 18. Measured and inverted Rrs scaled by a factor of 3 for spectral comparison to forward-modelled Rrs from Hydrolight. Notable differences can be seen, particularly between 350 and 555 nm, where poor atmospheric correction of ASD is suspected.

Multi-spectal Radiometer

Considering the major discrepancies between the reflectance measurements with the ASD and forward modeling from the IOPs, radiometric measurements from the multi-spectral OCR-507 radiometer were processed for comparison.

The OCR measures L_u at the DOLPHIN platform (ie. at depth) and E_d at the vessel deck. To reduce signal noise, data were median filtered to 10 cm depth bins.

L_u was then extrapolated to just below the sea-surface using 3 methods (below) which showed good correlation (figure 19). Extrapolated values are shown along the zero depth line.

1. Log transform L_u data (which should follow an exponential as $I = Io * e^{kz}$) and fit a line.
2. Calculate K_{lu} as :

$$K_{lu}(z') = -\ln(Lu(z+1) / Lu(z)) / (depth(z+1)-depth(z))$$

3. Use Hydrolight AOP (K_{lu})

Additional methods for L_u extrapolation, incluc the use of a cost minimization function for an exponential fit (Zaneveld, Boss et al. 2001) could be explored. Furthermore, normalization of the L_u to E_d should include a scaling factor over time, rather than using the mean E_d, as was done here.

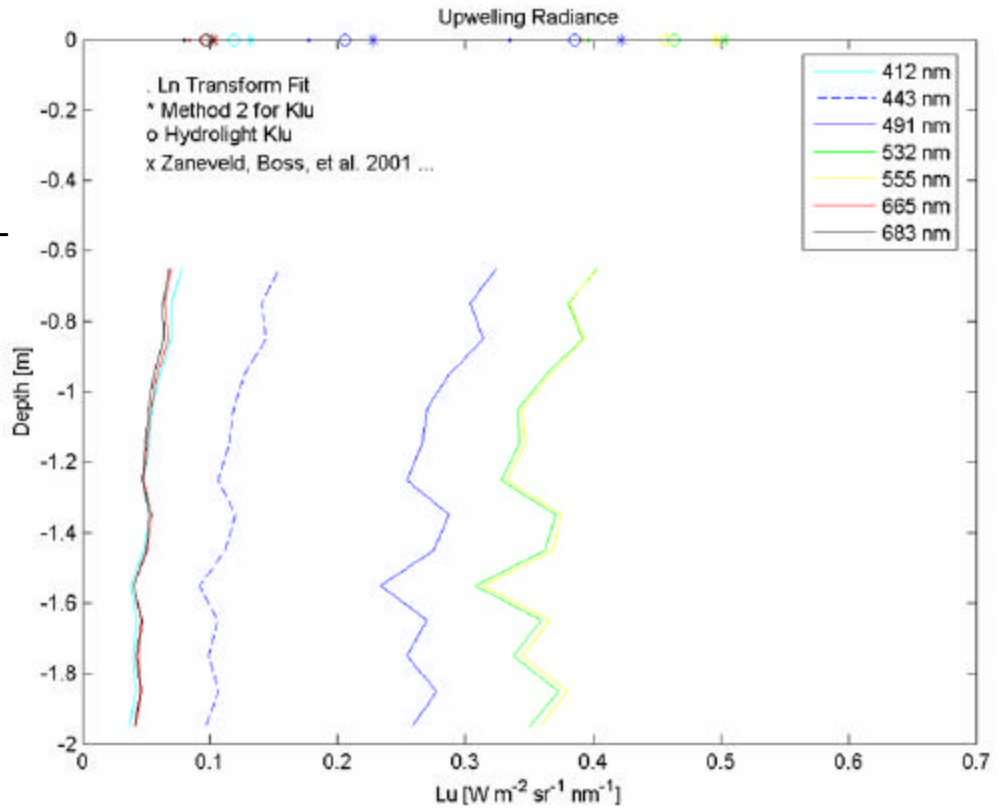

Figure 19. Extrapolation of upwelling irradiance to just below the sea-surface.

Subsurface L_u values were then propogated through the sea-surface to calculate Rrs using the empirical approximation that Lw = 0.54 Lu.

Extrapolated Irradiances

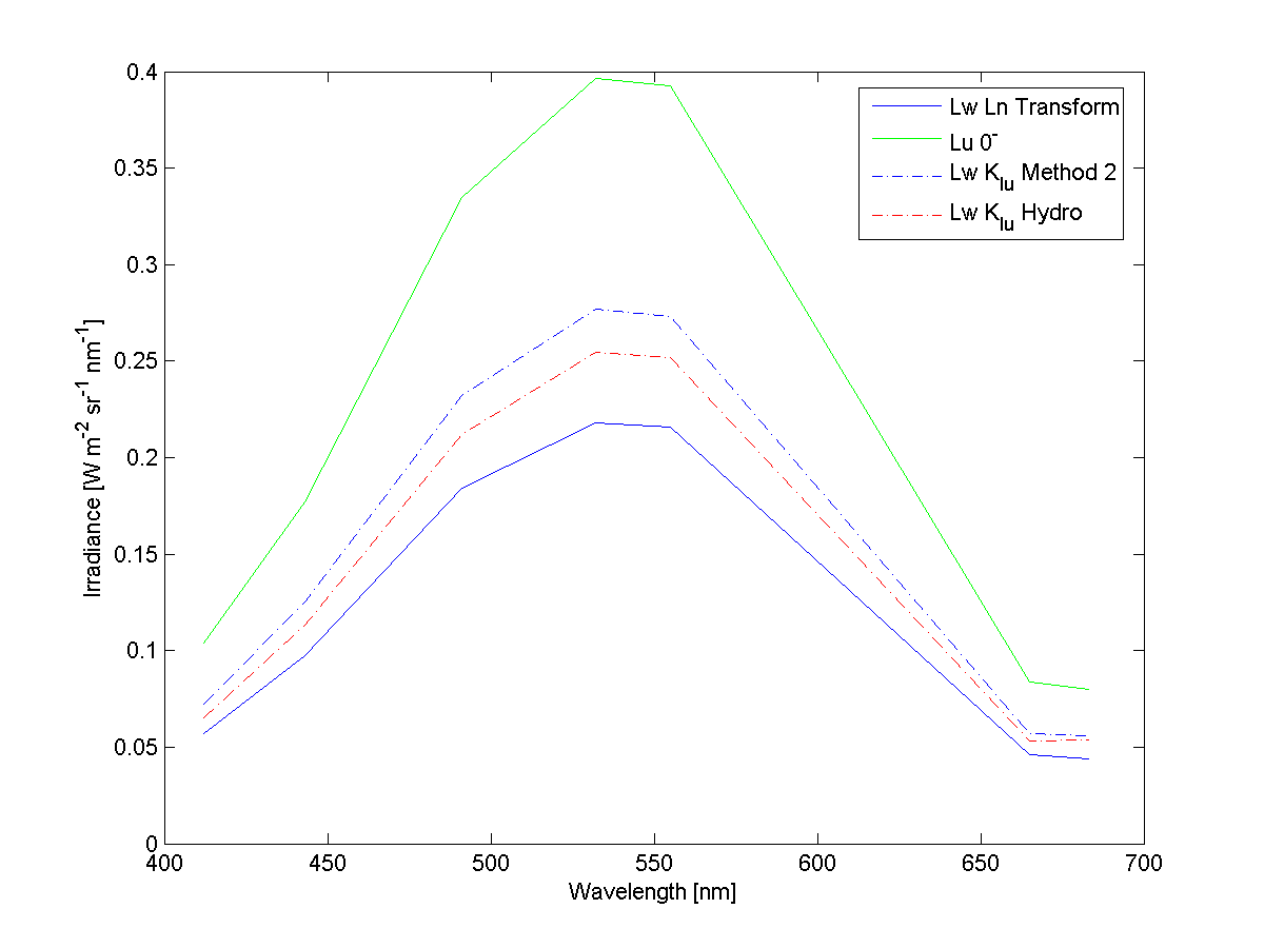

Figure 20. Extrapolated water-leaving irradiances shown spectrally with Lu (by natural log transform method) shown for comparison. Peak reflectance appears to be in the green, but fine spectral structure is lost with the multi-spectral instrument.

Comparison of OCR to ASD and Forward Model

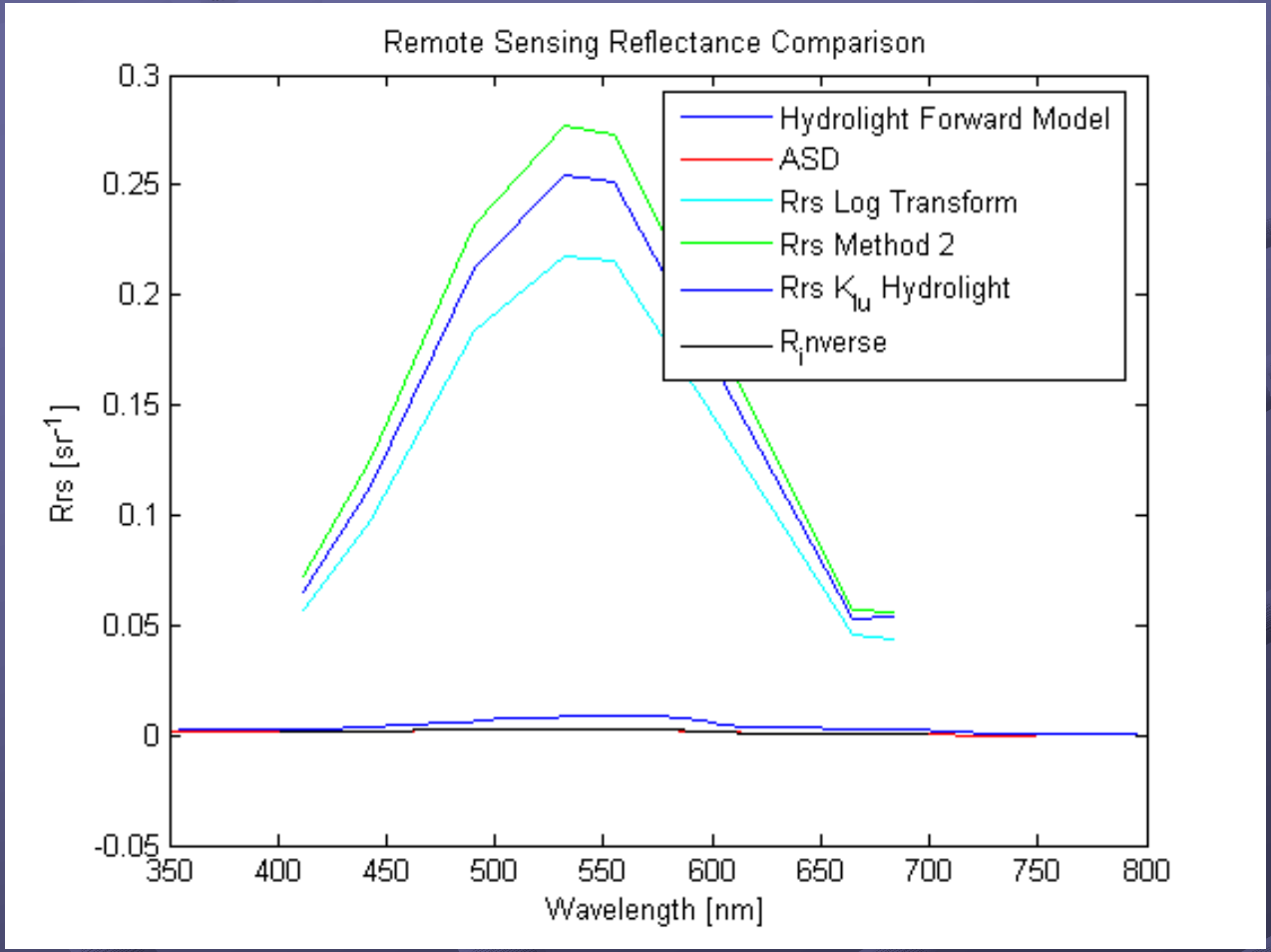

Figure 21. The calculated Rrs for the OCR differs from the Rrs of the ASD by as much as a factor of 92.3. It is possible that units of irradiance and radiance for the OCR were tabulated incorrectly.

Future Directions

- Establish radiometric instrument calibration and output (ie. units) first-hand
- Confirm the forward model of AOPs with an inversion of the Hydrolight forward model
- Fine-tune inversion model for location by application to more stations
- Seek out other radiometric measurements of the area for comparison (SeaWIFS, MODIS)